THE ASTRONOMICAL JOURNAL, 121:611–618, 2001 February

THE GRAVITATIONAL LENS CANDIDATE FBQ 1633+3134[1]

NICHOLAS D. MORGAN,[2] ROBERT H. BECKER,[3,4] MICHAEL D. GREGG,[3,4] PAUL L. SCHECHTER,[2] AND RICHARD L. WHITE[5]

Received 2000 July 19; accepted 2000 October 23

ABSTRACT

We present our ground-based optical imaging, spectral analysis, and high-resolution radio mapping of the gravitational lens candidate FBQ 1633+3134. This $z = 1.52$, $B = 17.7$ quasar appears double on CCD images with an image separation of 0.″66 and a relatively constant flux ratio of ~3:1 across B, V, R, and I filters. A single 0.27 mJy radio source is detected at 8.46 GHz, coincident within an arcsecond of both optical components, but no companion at radio wavelengths is detected for the system down to a flux level of 0.1 mJy (3 σ). Spectral observations reveal a rich metal-line absorption system consisting of a strong Mg II doublet and associated Fe I and Fe II absorption features, all at an intervening redshift of $z = 0.684$, suggestive of a lensing galaxy. Point-spread function subtraction of ground-based images however shows no obvious signs of a third object between the two quasar images and places a detection limit of $I \gtrsim 23.0$ if such an object exists. Although the possibility that FBQ 1633+3134 is a binary quasar cannot be ruled out, the evidence presented here is consistent with FBQ 1633+3134 being a single quasar lensed by a faint, metal-rich galaxy.

Key words: gravitational lensing — quasars: individual (FBQ 1633+3134)

1. INTRODUCTION

The number of quasars multiply imaged by gravitational lenses has steadily increased in the last decade. There are currently over 40 well-established cases of galaxy-size gravitational lenses (Kochanek et al. 1998). The usefulness of gravitational lenses is well known (Kochanek & Hewitt 1996). For example, measurements of a time delay between the light curves of individual images can lead to a determination of the Hubble constant (Refsdal 1964), while the observed frequency of strong-lensing events can provide statistical constraints on the cosmological constant (Kochanek 1996). Also, since the observed image configuration is sensitive to the gravitational potential of the lens, gravitational lensing offers a means to probe the matter distribution of the lensing object (e.g., Maller et al. 2000). This provides a method to sample the dark matter halos of intermediate-redshift galaxies that is independent of the galaxy's luminosity.

The mere identification of a close-separation (i.e., less than 10″) double quasar, however, is not confirmation of a gravitational lens. An alternative explanation is that the object is a physical binary quasar (e.g., Kochanek, Falco, & Mũnoz 1999; Mortlock, Webster, & Francis 1999). In principle, the distinction between these two possibilities is clear: either there is direct evidence for an intervening galaxy between the quasar images, confirming the lensing scenario, or the spectral properties of the pair differ to the extent that the most likely explanation is that there are two separate quasars. In the latter case, it is usually the failure to detect one of the quasars at radio wavelengths that eliminates the lensing hypothesis (e.g., Djorgovski et al. 1987; Muñoz et al. 1998). In practice, however, there are a number of quasar pairs that do not fall neatly into either category (Kochanek et al. 1999). The astrometric and spectral characteristics of these pairs are typical of gravitational lenses, yet no direct evidence for a lensing galaxy is found. The double quasar FIRST J163349.0+313412 (hereafter FBQ 1633+3134), which we analyze here, is best classified as one of these borderline systems. In this paper, we present our ground-based imaging, radio mapping, and spectral observations of FBQ 1633+3134 and discuss the likelihood that the system is a gravitational lens.

FBQ 1633+3134 ($16^h33^m48^s.97$, +31°34′11.″8 [J2000.0]) was originally identified as a $z = 1.52$, $B = 17.3$ quasar from the FIRST Bright Quasar Survey (FBQS; Gregg et al. 1996). The target was first detected as a 2 mJy radio source at 20 cm as part of the FIRST radio survey (Becker, White, & Helfand 1995), while follow-up spectral observations taken with the Lick 3 m telescope confirmed the radio source as a high-redshift quasar (White et al. 2000). The FBQS offers a major advantage over fainter quasar surveys for discovering lensed quasars. Since the majority of the FBQS targets are bright ($B < 18$), the probability of finding a quasar multiply imaged by gravitational lensing is enhanced over a sampling of fainter quasars because of the magnification bias effect (Turner, Ostriker, & Gott 1984). Using the 2.4 m Hiltner Telescope at the MDM Observatory, we have exploited this bias effect by obtaining optical images of the brightest ($B < 18$) and most distant ($z > 1$) of the FBQS quasars to search for arcsecond-scale multiple imaging indicative of strong gravitational lensing. One such observing run in 1996 December yielded the quasar FBQ 0951+2635 as a subarcsecond separation gravitational lens (Schechter et al. 1998). A subsequent observing run was carried out during 1997 June and targeted an additional 100 of the FBQS quasars in a further search for lenses. During this run, a 3 minute R-band exposure of FBQ 1633+3134

[1] Based on observations carried out in part at the MDM Observatory, the W. M. Keck Observatory, and the National Radio Astronomy Observatory (NRAO) Very Large Array. The NRAO is a facility of the National Science Foundation operated under cooperative agreement by Associated Universities, Inc.

[2] Department of Physics, Massachusetts Institute of Technology, Room 6-113, 77 Massachusetts Avenue, Cambridge MA 02139-4307; ndmorgan@mit.edu, schech@achernar.mit.edu.

[3] Department of Physics, University of California, Davis, 1 Shields Avenue, Davis, CA 95616-8677.

[4] Institute of Geophysics and Planetary Physics, Lawrence Livermore National Laboratory, P.O. Box 808, L-413, Livermore, CA 94551-9900; bob@igpp.ucllnl.org, gregg@igpp.ucllnl.org.

[5] Space Telescope Science Institute, 3700 San Martin Drive, Baltimore, MD 21218; rlw@stsci.edu.

revealed two stellar-like point sources separated by ~0.″7, while immediate follow-up exposures showed the same separation and similar flux ratios in the *B*, *V*, and *I* bandpasses as well, providing the initial evidence that FBQ 1633+3134 might be gravitationally lensed.

We describe our initial optical observations and analysis of FBQ 1633+3134 in § 2, as well as higher resolution follow-up optical imaging taken immediately afterward using the 3.5 m WIYN telescope. In § 3, we describe the original FBQS spectrum taken of FBQ 1633+3134, as well as follow-up spectral observations taken with the Keck 10 m telescope. While radio observations were originally obtained as part of the FIRST survey, we have since obtained higher resolution Very Large Array (VLA) radio imaging of FBQ 1633+3134, following the optical detection of the object's double nature. We present these radio observations and their implications in § 4. Finally, we discuss lens modeling and interpretation of the system in § 5, while § 6 summarizes our findings and conclusions for FBQ 1633+3134.

2. OPTICAL OBSERVATIONS AND REDUCTION

2.1. *Initial Optical Imaging*

Initial optical images of FBQ 1633+3134 were taken by one of us (P. L. S.) with the MDM 2.4 m Hiltner Telescope as part of the optical follow-up program for FBQS quasars described above. Imaging was conducted on the nights of 1997 June 1, 2, and 4. The Tek 1024 × 1024 CCD detector ("Charlotte") was used, with a gain of 3.16 e^- ADU^{-1} and a read noise of 5.45 e^-. The telescope was operated at an f ratio of f/7.5, yielding a plate scale of 0.″2750 pixel^{-1}. Sky conditions were marred by the presence of intermittent clouds on the nights of June 2 and 4, although observations reported here were taken during photometric periods. Multiple 3 minute exposures of FBQ 1633+3134 were taken using the Schombert *BVRI* filter set, with seeing conditions that ranged from 0.″8 to 1.″0 FWHM. Multiple *BVRI* observations of the Landolt standard field PG 1633 (Landolt 1992) were also taken on the night of June 2. A summary of the MDM observations for FBQ 1633+3134 are presented in Table 1. Figure 1 shows a 5′ square field of the target quasar and nearby stars from one of the *I*-band frames.

All CCD frames were bias-subtracted, flattened, and trimmed using the VISTA reduction program. The flat-field frames consisted of twilight sky exposures taken on June 1, and cosmic rays were removed by using AUTOCLEAN, a program written and kindly provided by J. Tonry. The initial 3 minute *R*-band exposure of FBQ 1633+3134 showed it to be noticeably misshapen as compared with other stars in the field, with an ellipticity of ~0.6 (Fig. 2, *top left*). This large ellipticity is consistent with a comparatively bright companion less than an arcsecond away from the brighter optical component. There is also a faint point source ~3″ to the southwest of the elongated image, with a peak flux of ~1 % of the peak flux of the target quasar.

TABLE 1

SUMMARY OF MDM OBSERVATIONS, 1997 JUNE

Filter	N_{img}	Average FWHM
B	5	1.″00
V	12	0.″82
R	4	0.″87
I	8	0.″87

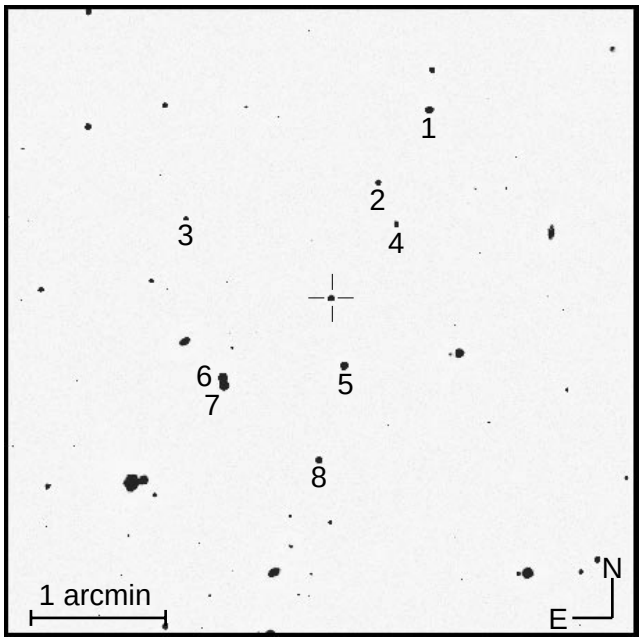

FIG. 1.—*I*-band 3 minute exposure of FBQ 1633+3134 (*center crosshairs*) and surrounding field. North is up and east is to the left. The scale of the image is shown at bottom left.

Preliminary photometry for the MDM data was performed using the DoPHOT package (Schechter, Mateo, & Saha 1993), which was able to split FBQ 1633+3134 as a double image in all bandpasses. We fitted the elongated image with two empirical point-spread functions (PSFs), using a variant of the DoPHOT program designed to deal with close, pointlike, and extended objects (Schechter & Moore 1993). Hereafter we will refer to the brighter and fainter components of the two PSF fits as components A and B, respectively. We simultaneously fitted for the presence of the faint southwestern object as well (hereafter, component C), to ensure that this object did not affect the photometric solutions for the main components. Star 5 in Figure 1 served as the empirical PSF template.

For our photometric fits presented here, we have simultaneously solved for the relative fluxes of the system components and the overall position of the system but have held the relative separations of the components fixed at values determined from *Hubble Space Telescope* (*HST*) Near Infrared Camera and Multi-Object Spectrometer (NICMOS) imaging of E. Falco (principal investigator), obtained as part of the CASTLES program (Kochanek et al. 1998) in 1998 August.[6] Using the archival *HST* NICMOS images of FBQ 1633+3134, centroid positions for components A, B, and C were fitted by the authors, using Gaussian fits to the peaks of the flux profiles, which gave a separation between the brighter two components of 0.″663. Appropriate steps were then taken to account for the relative orientations and plate scales of the MDM and *HST* NICMOS detectors. We report our photometric solutions for the MDM data using

[6] The *HST* NICMOS images of FBQ 1633+3134 may be viewed online at the CASTLES homepage at http://cfa-www.harvard.edu/castles.

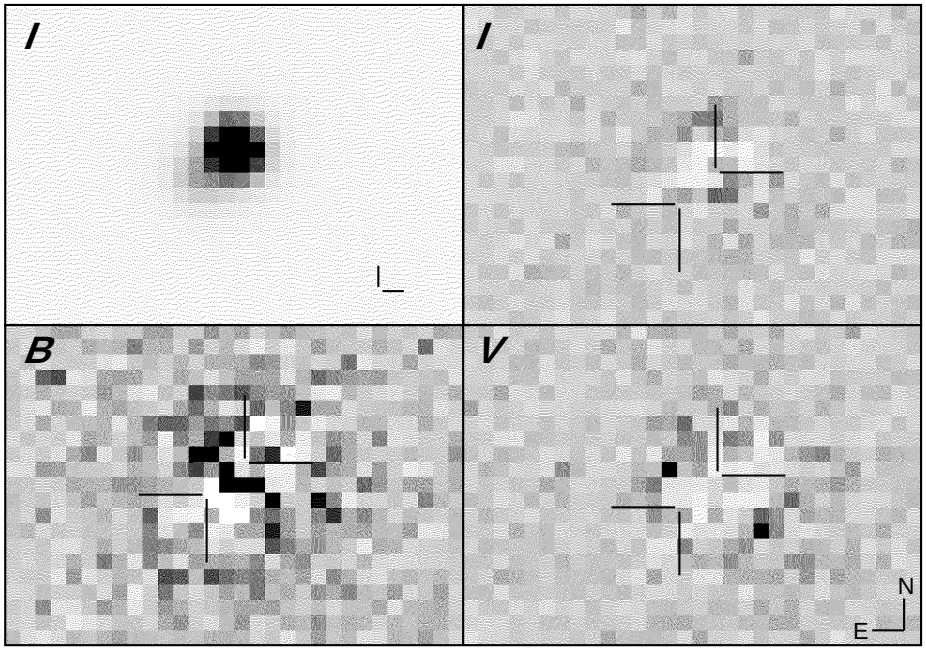

FIG. 2.—Extracted subrasters of FBQ 1633+3134 taken with the WIYN 3.5 m telescope. North is up and east is to the left. Each panel is ~4″ wide. *Top left*: A 120 s *I*-band exposure, showing component A in the northwest and component B in the southeast. The small tick mark southwest of the pair indicates the centroid location of component C (which is too faint to be seen at the given contrast level). *Top right*: *I*-band residuals from two-component empirical PSF subtraction of components A and B. Tick marks indicate the centroid location of the two components. *Bottom left*: Stacked *B*-band residuals from two-component PSF subtraction. *Bottom right*: *V*-band residuals from two-component PSF subtraction. The saturation levels for the residual panels are at $\pm 10\ \sigma$, where σ is the respective rms sky noise for each image. Component A has a peak intensity of $\sim 580\ \sigma$, $\sim 482\ \sigma$, and $\sim 420\ \sigma$ for the *B*- (stacked), *V*-, and *I*-band exposures, respectively.

fixed relative positions for the three components of the system in Table 2. Error bars in Table 2 are statistical (1 σ) errors obtained from the frame-to-frame scatter for each filter.

It can be seen that the broadband magnitude differences between components A and B show relatively little variation across wavelength. The photometric solutions reported in Table 2 correspond to $A:B$ flux ratios of 2.45, 3.25, 3.24, and 3.36 in *B*, *V*, *R*, and *I*, respectively. This is consistent with components A and B having similar spectral energy distributions (SEDs) at optical wavelengths, as would be expected if the system consisted of two quasars (Mortlock et al. 1999) or a single quasar multiply imaged by gravitational lensing. Component B has a $B-V$ color index of 0.114 and $V-R$ and $V-I$ color indexes of 0.356 and 0.691 with uncertainties of ~ 0.04 for each index. The $B-V$ index is consistent with an A star, while the $V-R$ and $V-I$ indexes are consistent with a late F to early G star. The color of component B is therefore inconsistent with it being a foreground Galactic star. The $B-V$, $V-R$, and $V-I$ color indexes for component A are 0.422, 0.353, and 0.725 with uncertainties of ~ 0.02 for each index. Although these colors are consistent with a late F star, spectral observations presented in § 3 make it highly unlikely that the brighter component is a Galactic star.

The photometric solutions reported in Table 2 also shed light on the nature of component C. Component C has $B-V$, $V-R$, and $V-I$ color indexes of 0.95, 0.50, and 0.95, respectively, with (1 σ) statistical errors of ~ 0.2 for $B-V$ and ~ 0.1 for $V-R$ and $V-I$. These colors are consistent with a late G to early K star. In addition, if we suppose components A and B do indeed arise from gravitational lensing, then the position of component C relative to components A and B is inconsistent with it being either a third image of the lensed quasar or the lensing galaxy. Because it also appears as a point source in our optical imaging, we conclude that component C is a foreground Galactic star and is not physically associated with the two brighter components of the system.

2.2. *Astrometry and Photometric Calibration*

The apparent magnitudes for FBQ 1633+3134 reported in Table 2 were calibrated using offsets and color terms obtained from observations of the Landolt standard field

TABLE 2

MDM PHOTOMETRIC SOLUTIONS FOR FBQ 1633+3134

Comp.	Δ R.A.	Δ Decl.	*B*	*V*	*R*	*I*
A.....	...	...	18.046 ± 0.017	17.624 ± 0.006	17.271 ± 0.013	16.899 ± 0.010
B.....	0.″524	−0.″406	19.019 ± 0.033	18.905 ± 0.019	18.549 ± 0.037	18.214 ± 0.034
C.....	−1.″793	−2.″282	23.268 ± 0.167	22.315 ± 0.071	21.814 ± 0.037	21.370 ± 0.063

NOTE.—Relative astrometric positions were obtained from the archival CASTLES *HST* NICMOS imaging. Magnitude solutions for the MDM data were obtained while holding the relative separations fixed at the *HST* values. Error bars are statistical (1 σ) and do not include uncertainties in the PSF star calibration. See note to Table 3.

PG 1633 (Landolt 1992), where we have used extinction coefficients taken from the Kitt Peak direct imaging manual ($k_B = 0.25$, $k_V = 0.15$, $k_R = 0.10$, and $k_I = 0.07$; Massey et al. 1997). The fitting program described above yields flux ratios for all objects in the field with respect to the PSF template star. Once the PSF star has been calibrated onto the standard system, obtaining apparent magnitudes for the remaining objects in the field is straightforward. We have also obtained astrometric solutions for reference objects in the field relative to the Automatic Plate Measuring (APM) astrometry of McMahon & Irwin (1992), using one of the *I*-band frames. To aid in the calibration of future observations, Table 3 presents our photometric and astrometric solutions for eight reference stars within a 5arcmin radius of the target quasar. The positional uncertainties in the astrometric solutions are 0.″4 (1 σ).

2.3. *Follow-up Optical Imaging*

To probe components A and B for possible signs of a lensing galaxy, higher resolution follow-up imaging of FBQ 1633+3134 was taken by C. Bailyn immediately following the MDM run. On 1997 June 5, a total of six CCD exposures of FBQ 1633+3134 were taken (two each in Harris *B* and *R*, and one each in *V* and *I*) using the WIYN 3.5 m telescope at the Kitt Peak National Observatory. The 2SKB 2048 × 2048 detector was used, with a gain setting of 2.8 e^- ADU^{-1}, a read noise of 8 e^-, and a plate scale of 0.″1971 pixel^{-1}. Seeing conditions for the series of exposures were 0.″7 FWHM, significantly better than for the MDM run. Each exposure lasted 120 s. These images were bias-subtracted, flattened, and trimmed using standard IRAF procedures, and the *B*- and *R*-band images were stacked using integer-pixel offsets before obtaining photometric solutions. PSF fitting was then carried out using the identical procedure as for the MDM data, with star 5 again providing the empirical PSF template.

Results from PSF analysis, again using fixed relative positions taken from the *HST* NICMOS data, yield A:B flux ratios of 2.67, 3.20, 3.21, and 3.28 in *B*, *V*, *R*, and *I*, respectively. These results agree well with the corresponding MDM flux ratios for the two components. In Figure 2, we show an excised portion of the *I*-band frame, along with residuals after empirical PSF subtraction for the *V* and *I* filters. Tick marks for the residual panels indicate the centroid locations of components A (northwest) and B (southeast); the orientation of the system is identical in all four panels. We do not show the *R*-band residuals, as the *R*-band PSF was discovered to vary slightly over the face of the detector, which masked any residual signature from FBQ 1633+3134 that may have been present because of additional sources of flux in the system. The ellipticity of the *R*-band PSF increased from ~0.01 to ~0.06 for stars sampled from the center to the periphery of the detector, leaving an FBQ 1633+3134 residual pattern that is ~1 % of component A's brightness. The *R*-band PSF-induced residual pattern seen for components A and B of FBQ 1633+3134 was similar to the patterns observed for isolated stars in the field.

Visual inspection of our ground-based *B*-, *V*-, and *I*-band residuals shows no obvious sign of unaccounted-for flux in the system. Although we did not perform a rigorous PSF subtraction of the *HST* NICMOS data, a cursory inspection of the CASTLES image also shows no obvious indication of a lensing galaxy. If a lensing galaxy were located between components A and B, its presence would be most evident in our ground-based images in *I* band, where the quasar-galaxy flux contrast would be more nearly equal. To quantify the *I*-band magnitude limit for our nondetection, we have inserted a series of Gaussian flux profiles, representative of an intervening galaxy, between components A and B and investigated the residual patterns that emerged after fitting and subtracting two empirical PSFs as described above. The location of the Gaussian profile was dictated by the singular isothermal sphere model (see § 5), with an FWHM of 0.″71 (the average seeing for the *I*-band exposure). Again holding the relative separations of components A and B fixed at the *HST* NICMOS values, we were able to detect 5 σ residuals for a third object down to $I = 23.0$, where σ is the rms sky noise of the exposure. We therefore confidently rule out the presence of an $I < 23$ mag point source at the suspected lensing galaxy position. The significance of this nondetection is discussed in § 5.

3. SPECTROSCOPY

A spectrum of FBQ 1633+3134 had been originally obtained by one of us (R. B.) using the Kast Double Spectrograph at the Lick Observatory on 1996 June 10 as part of the FIRST Bright QSO Survey (see White et al. 2000). The spectrum left no doubt that FBQ 1633+3134 was a quasar, clearly showing redshifted C IV, C III, and Mg II emission features. Several metal-line absorption features were also detected from an intervening line-of-sight

TABLE 3

RELATIVE ASTROMETRY AND APPARENT MAGNITUDES FOR FIELD STARS

Object	Δα (s)	Δδ (arcsec)	*B*	*V*	*R*	*I*
1	−3.010	115.11	18.299 ± 0.002	17.128 ± 0.001	16.407 ± 0.001	15.827 ± 0.002
2	−1.206	82.37	19.158 ± 0.002	18.537 ± 0.003	18.215 ± 0.002	17.864 ± 0.003
3	5.580	66.18	20.557 ± 0.006	19.296 ± 0.002	18.489 ± 0.002	17.775 ± 0.003
4	−1.829	63.61	19.853 ± 0.001	18.605 ± 0.002	17.776 ± 0.002	17.058 ± 0.002
5	0.000	0.00	18.670 ± 0.000	17.187 ± 0.000	16.059 ± 0.000	14.673 ± 0.000
6	4.275	−5.35	17.200 ± 0.002	16.225 ± 0.001	15.708 ± 0.001	15.242 ± 0.002
7	4.216	−8.93	17.556 ± 0.003	16.417 ± 0.001	15.729 ± 0.001	15.108 ± 0.002
8	0.885	−42.38	18.702 ± 0.003	17.810 ± 0.001	17.339 ± 0.002	16.904 ± 0.002

NOTE.—Object numbers correspond to the labels shown in Figure 1. Reported error bars are statistical (1 σ) errors from the observed dispersion between frames and do not include uncertainties in the calibration of the PSF star (object 5). Magnitude uncertainties (1 σ) for the PSF star are 0.007, 0.008, 0.005, and 0.004 for the *B*, *V*, *R*, and *I* filters, respectively, and must be added in quadrature to the errors reported above.

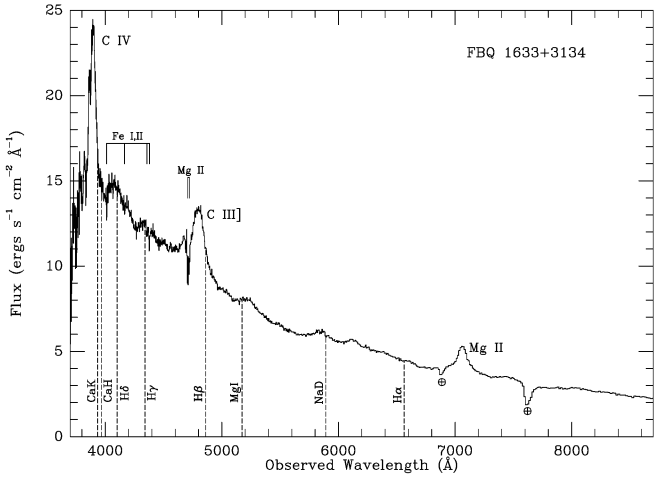

FIG. 3.—Composite spectrum of FBQ 1633+3134 A, B taken with the Keck 10 m telescope. Integration time was 600 s. Prominent emission features are indicated for this $z = 1.52$ quasar, as well as the identification of a $z_{abs} = 0.684$ metal-rich absorption system. Also identified in the original Lick spectrum (not shown here) are the Ca I λ2201 and the Fe I λ2984 absorption features, at redshifts $z_{abs} = 0.685$ and $z_{abs} = 0.684$, respectively. The lack of any stellar absorption features at the indicated wavelengths (*dashed lines*) argues against either component being a foreground Galactic star.

absorber. However, the signal-to-noise ratio (S/N) of the Lick spectrum was only ~10 at blue wavelengths, which hampered the absorption analysis.

We have since obtained a higher S/N spectrum using the Echellette Spectrograph and Imager (ESI; Epps & Miller 1998) at the Keck Observatory on 2000 March 9. The wavelength range of the observations was from 3700 to 8700 Å, with a dispersion that ranged from 0.7 to 11 Å from blue to red wavelengths. The slit orientation was held at P.A. 40° east of north, roughly perpendicular to the image separation. The seeing FWHM was 0.″8, insufficient to resolve the two components. The 600 s spectrum is shown in Figure 3.

We present our identification of prominent absorption and emission features for the FBQ 1633+3134 spectrum in Table 4. The source quasar has a redshift of 1.513 (2) based on Gaussian fits to peaks of the C III and C IV emission features. The S/N of the Keck spectrum ranges from ~50 to ~90 from blue to red wavelengths, allowing the confident

TABLE 4

SPECTRAL ANALYSIS FOR FBQ 1633+3134

Species	λ_{obs}	λ_{rest}	z
Emission:			
C IV	3889.9	1549.3	1.5107 (5)
C III	4799.7	1908.7	1.5146 (11)
Mg II.....	7064.4	2799.5	1.5235 (5)
Absorption:			
Ca I	3708.9	2201.4	0.6848 (4)
Fe II.....	4012.0	2382.8	0.6837 (2)
Fe I	4165.8	2473.9	0.6839 (3)
Fe II.....	4354.8	2586.7	0.6836 (2)
Fe II.....	4377.9	2600.2	0.6837 (1)
Mg II.....	4707.5	2796.4	0.6834 (3)
Mg II.....	4719.8	2803.5	0.6835 (1)

NOTE.—Numbers in parenthesis are 1 σ error bars.

detection of an intervening metal-line absorption system at $z_{abs} = 0.684$. The Mg II $\lambda\lambda$2796, 2803 doublet is clearly resolved in Figure 3, as is a series of Fe II $\lambda\lambda$2383, 2586, 2600 and Fe I λ2474 absorption lines. The Mg II doublet has a total rest-frame equivalent width of 2.4 Å. A strong (1.7 Å equivalent width) absorption feature at an observed wavelength of λ3708.9 was also detected in the Lick spectrum, which may correspond to Ca I λ2201 at the slightly higher redshift of $z_{abs} = 0.685$. The detection of a strong Mg II and Fe absorption system is evidence that there may exist a damped Lyman α system (DLAS) at the absorber redshift. A DLAS at intermediate redshift is likely to be the dusty, metal-rich disk of a late-type galaxy (Boisse et al. 1998).

The high S/N of the Keck spectrum provides a means to rule out the possibility that either component is a Galactic star. In general, the equivalent width of a spectral absorption feature is reduced by a factor of $(1 + f)^{-1}$ when flooded with continuum flux from a companion object, where f represents the ratio of continuum intensities of the brighter object to the fainter object exhibiting the absorption feature. Prominent stellar absorption features typically have equivalent widths that are of order 1 Å (Jacoby, Hunter, & Christian 1984). Thus, if the fainter optical component was indeed a Galactic star, the 3:1 optical flux ratio would predict stellar absorption features of typical equivalent width 0.25 Å. The equivalent width associated with the rms noise in the Keck spectrum ranges from 0.01 Å in the blue to 0.1 Å in the far red. The Keck spectrum therefore has an S/N high enough to detect stellar absorption features confidently if they were present. None of the common stellar absorption features are detected at the indicated positions (*dashed lines*) of Figure 3, which argues against either component being a foreground Galactic star. The simplest explanation for the combined spectrum is that we are seeing the light from two identical-redshift quasars.

4. RADIO OBSERVATIONS

FBQ 1633+3134 is a millijansky radio source at 20 cm in the FIRST survey. The survey was carried out using the Very Large Array in the B configuration, providing a resolution of ~5″ (Becker et al. 1995). The original radio observations lack the required resolution to probe for subarcsecond companions to the target quasar. Once optical observations had revealed the quasar's double nature, higher resolution VLA imaging was obtained.

On 1998 March 14, follow-up VLA observations of FBQ 1633+3134 were carried out by one of us (R. B.) at 8.46 GHz while the VLA was in the A configuration, providing an angular resolution of 0.″2. Integration time was 60 minutes. Only one source was securely detected, with a peak intensity of 0.27 mJy and an rms noise level in the field of 0.03 mJy.

If we assume the radio emission comes from the brighter component of the optical pair, then the optical flux ratio of ~3:1 would predict a peak radio intensity of ~0.1 mJy for the fainter component. The failure to detect a radio component is therefore significant at the 3 σ level.

The position of the radio source from the high-resolution VLA imaging was determined to be ($16^h33^m48^s.943$, $+31°34'11''.19$ [J2000.0]), with a positional uncertainty of ~0.2″. This differs from our ground-based optical positions of component A, ($16^h33^m48^s.974$, $+31°34'11''.85$), by 0.″8 and for component B, ($16^h33^m49^s.020$, $+31°34'11''.44$), by 1.″0. The APM catalog position for the composite AB source

shows the same difference. We also queried the US Naval Observatory A2.0 (USNO-A2.0) catalog, which uses the Precision Measuring Machine astrometry of Monet et al. (1996), and found a similar 1.″0 offset with respect to the radio position. We are therefore unable to identify with confidence which of the two optical components corresponds to the radio detection. We note that a similar 1″ discrepancy between VLA and optical astrometric solutions was also identified for the FIRST lensed quasar FBQ 0951+2635 (Schechter et al. 1998).

5. MODEL AND INTERPRETATION

The identification of an intervening metal-line absorption system in the FBQ 1633+3134 spectrum raises the obvious question of whether this material could serve as the lens. Although this possibility is attractive from the lensing point of view, the mere presence of an intervening absorption system should not be taken as direct evidence of a lensing galaxy. The observed incidence of Mg II absorption systems in quasar spectra is about one such system per unit redshift range down to a minimum equivalent width of 0.3 Å (Steidel & Sargent 1991), so it is common to find an intervening metal-line absorber in the spectra of high-redshift quasars. In this section, we explore the likelihood that the $z_{\rm abs} = 0.684$ absorber could indeed indicate the presence of the lensing galaxy and investigate the properties of the putative lensing galaxy as constrained by other observables of the system. Throughout this section, we have adopted an $\Omega_m = 0.3$, $\Omega_\Lambda = 0.7$ cosmological model and have parameterized the Hubble constant as $H_0 = 100\,h$ km s^{-1} Mpc^{-1}.

We will adopt the singular isothermal sphere (SIS) model to describe the gravitational potential of the hypothesized lensing galaxy. The SIS model is fully described by the line-of-sight velocity dispersion σ of the lensing galaxy. The corresponding Einstein radius is $\Theta_{\rm E} = 4\pi(\sigma/c)^2 D_{\rm LS}/D_{\rm OS}$, where $D_{\rm LS}$ and $D_{\rm OS}$ are the angular diameter distances from the lens to the source and from the observer to the source, respectively (e.g., Narayan & Bartleman 1998). The SIS produces a two-image lens configuration with an angular separation of $2\Theta_{\rm E}$ between the two images. If the angular distance between the brighter (fainter) image and the core of the potential is denoted by AG (BG), then the ratio of image distances AG/BG is the same as the lensing-induced flux ratio of the two images. We further take the B-band luminosity of galaxies to be related to their line-of-sight velocity dispersions according to a Faber-Jackson relationship (1976) of the form $L/L_* = (\sigma/\sigma_*)^\gamma$. Following Keeton, Kochanek, & Falco (1998), we adopt parameters of $\sigma_* = 220$ (144) km s^{-1} and $\gamma = 4$ (2.6) for early-type elliptical galaxies (late-type spiral galaxies), where L_* corresponds to a B-band magnitude of $M_B^* = -19.7 + 5 \log h$.

For a given lensing redshift z_l, one can use the observed image separation to estimate the velocity dispersion and luminosity of the lensing galaxy. Figure 4 shows the predicted lensing galaxy's luminosity as a function of redshift for both an early-type elliptical and a late-type spiral. At the redshift of the metal-line absorber (Fig. 4, *dashed line*), the predicted luminosities for both galaxy types are comparable an L_* galaxy: $\sim 0.3L_*$ for the elliptical and $\sim 1.3L_*$ for the spiral, with a corresponding dark matter velocity dispersion of ~ 160 km s^{-1} for both galaxy types. The observed image separation can therefore be reproduced by a slightly overluminous spiral or underluminous elliptical (with respect to an L_* galaxy) at the absorber redshift. We also use the techniques of Kochanek (1992) to estimate the lens redshift probability distribution for the system. Using a critical lens radius of $r = 0.''33$ for FBQ 1633+3134, we compute a median redshift for an elliptical (spiral) lens galaxy of $z = 0.72$ (0.59), with a 2 σ redshift interval of $0.21 \lesssim z \lesssim 1.15$ ($0.17 \lesssim z \lesssim 1.04$). The detected metal-line absorption at $z_{\rm abs} = 0.684$ lies within 1 σ of the median lensing redshift for either type of galaxy.

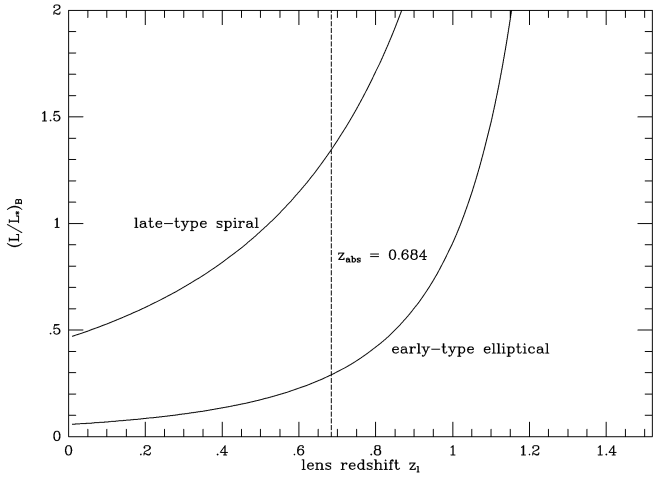

FIG. 4.—Predicted B-band luminosity (in units of L_*) of the hypothesized lensing galaxy as a function of its lensing redshift, z_l. Results for a late-type spiral galaxy and an early-type elliptical galaxy are shown. The redshift of the intervening absorption system is indicated by the vertical line. The corresponding central velocity dispersion at the absorber redshift is ~ 160 km s^{-1}.

Although the redshift and predicted velocity dispersion of any intervening galaxy are consistent with gravitational lensing, the predicted luminosity of the lens is difficult to reconcile with the detection limits presented in § 2. Using SEDs for early- and late-type galaxies, we predict the apparent magnitude of the lensing galaxy as a function of the lensing redshift, z_l. To calculate broadband apparent magnitudes, we adopt SEDs from S. Lilly (1997, private communication), that consist of interpolated and extrapolated curves from Coleman, Wu, & Weedman (1980). No evolution correction was applied to the energy distributions. The SEDs were normalized to their Faber-Jackson B-band luminosities at $4400(1 + z_l)$ Å, which yields the predicted absolute magnitudes on the AB magnitude system. The corresponding apparent magnitudes are then computed using the cosmological distance modulus relation

$$m_{\rm AB}(\lambda_{\rm obs}) - M_{\rm AB}(\lambda_{\rm rest}) = 5 \log \left(\frac{D_L}{10\ {\rm pc}} \right) + 7.5 \log (1 + z_l)\ , \quad (1)$$

where D_L is the angular diameter distance to the lensing galaxy. The apparent AB magnitudes are finally transformed onto the standard $BVRI$ system by subtracting -0.110, 0.011, 0.199, and 0.456, respectively (Fukugita, Shimasaku, & Ichikawa 1995). The resulting magnitudes are probably uncertain by as much as ± 1 mag.

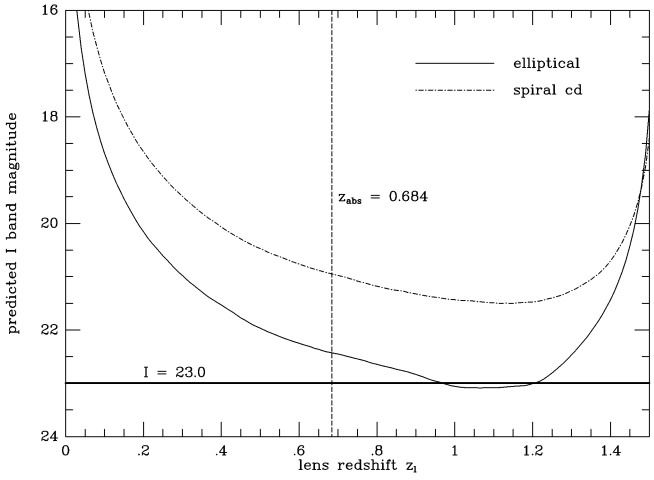

FIG. 5.—Predicted I-band apparent magnitudes of the hypothesized lensing galaxy as a function of its lensing redshift, z_l. Results are shown for a late-type spiral galaxy (*dot-dashed line*) and an early-type elliptical galaxy (*solid line*). The $I = 23.0$ detection limit for any such galaxy is indicated by the horizontal line, and the redshift of the intervening absorption system is shown by the vertical line.

Figure 5 presents our I-band magnitude predictions for both an early-type elliptical and a late-type spiral galaxy as a function of lensing redshift. The predicted apparent magnitudes initially become fainter with increasing redshift, but they eventually increase to brighter magnitudes as the lens redshift approaches the source redshift. This increase is because the velocity dispersion required to produce a fixed image separation increases without bound as the lens approaches the source, leading to a corresponding increase in the lens luminosity. For FBQ 1633+3134, the I-band detection limit of $I = 23$ from § 2 roughly corresponds to the faintest predicted magnitude for an early-type elliptical, but it is $\sim$1.5 mag fainter than the faintest prediction for a late-type spiral. At the absorber redshift of $z_{abs} = 0.684$, the predicted magnitudes lie above the detection limit by $\sim$0.5 ($\sim$2.0) mag for an elliptical (spiral) galaxy. While an early-type elliptical lensing galaxy could conceivably escape our I-band detection limit, a late-type spiral should have been bright enough to detect in our optical imaging.

6. SUMMARY AND CONCLUSIONS

From an observational standpoint, the requirements for a double quasar to be confidently classified as a gravitational lens can be stated as follows: First, since gravitational lensing is achromatic, the optical flux ratio of the components should (ideally) be self-consistent across broadband filters. In practice, however, the ratios will not agree exactly because of differential reddening through the lens galaxy (McLeod et al. 1998) and microlensing by stars in the lens galaxy (Wisotzki et al. 1993). More importantly, the radio flux ratio, if available, must also agree with the optical ratio, again because of the achromatic nature of lensing. Second, spectral observations of the quasar pair must support the conclusion that both objects are identical-redshift quasars with similar (although not necessarily identical; Wisotzki et al. 1993) emission and continuum properties. Third, the lensing galaxy itself must be detected, ideally by direct imaging, although weaker arguments based on the presence of intervening absorption features in the QSO spectrum have been used in the past (e.g., Hewett et al. 1994). In practice, the first two requirements are necessary for a lens classification, while the third (direct imaging of the lensing galaxy) is usually sufficient.

FBQ 1633+3134 meets the necessary requirements for a gravitational lens. The broadband flux ratio ($\sim$2.5:1 in B, $\sim$3.3:1 in V, R, and I) is self-consistent across broadband wavelengths. Although only one component was detected in radio, the lower limit to the radio flux ratio of $\gtrsim$3:1 is not in severe conflict with the corresponding optical flux ratio. Also, the spectral analysis argues against either component of the pair being a Galactic star, while the unresolved emission profiles from the pair are consistent with two identical-redshift quasars.

Unfortunately, the sufficient condition that could elevate FBQ 1633+3134 to the status of a lensed quasar, direct detection of the lensing galaxy, is not realized with our optical imaging. Subtraction of two PSFs for the WIYN data presented in § 2 shows no significant indication of unaccounted-for flux in the system and places a magnitude limit of $I > 23.0$ by using a simple SIS model for the lensing potential. Although the hypothesized lens galaxy is not detected directly, a weaker argument for its presence can be made from the spectral identification of a rich $z_{abs} = 0.684$ metal-line absorption system, which is within 1 σ of the median lensing redshift. Also, the estimated luminosity of the suspected galaxy does not differ strongly from an L_* galaxy for either of the galaxy types considered here. On the other hand, the predicted apparent magnitude of a late-type spiral at the absorber redshift is $\sim$2 mag above the I-band detection threshold, while an early-type galaxy is only marginally consistent with the detection limit.

We conclude that FBQ 1633+3134 is a strong candidate for a close-separation (0.″66) gravitational lens. The evidence presented here suggests lensing by a relatively faint ($I > 23.0$), $z = 0.684$ metal-rich galaxy, although the binary quasar scenario cannot be positively ruled out. Confirmation of the lensing hypothesis can be provided by a deeper radio probe for the fainter component of the system. We have obtained VLA A array time for late 2000 with this aim in mind and intend to present these results, along with a systematic analysis of the *HST* data for this system, in a future paper.

The authors would like to thank Charles Bailyn for obtaining the WIYN optical data of FBQ 1633+3134 and Brian Skiff for noticing a V-band calibration error in an earlier version of this paper. N. D. M. and P. L. S. gratefully acknowledge the support of the National Science Foundation through grant AST 96-16866. Some of the data presented here were obtained at the W. M. Keck Observatory, which is operated as a scientific partnership among the California Institute of Technology, the University of California, and the National Aeronautics and Space Administration. The Keck Observatory was made possible by the generous financial support of the W. M. Keck Foundation. The FIRST Survey is supported by the National Science Foundation through grant AST 98-02791 and by NATO, the National Geographic Society, Sun Microsystems, and Columbia University. Part of the work reported here was done at the Institute of Geophysics and Planetary Physics under the auspices of the Department of Energy at the Lawrence Livermore National Laboratories under contract W-7405-Eng-48.

REFERENCES

Becker, R. H., White, R. L., & Helfand, D. J. 1995, ApJ, 450, 559
Boissé, P., Le Brun, V., Bergeron, J., & Deharveng, J.-M. 1998, A&A, 333, 841
Coleman, G. D., Wu, C. -C., & Weedman, D. W. 1980, ApJS, 43, 393
Djorgovski, S., Perley, R., Meylan, G., & McCarthy, P. 1987, ApJ, 321, L17
Epps, H. W., & Miller, J. S. 1998, Proc. SPIE, 3355, 48
Faber, S. M., & Jackson, R. E. 1976, ApJ, 204, 668
Fukugita, M., Shimasaku, K., & Ichikawa, T. 1995, PASP, 107, 945
Gregg, M. D., Becker, R. H., White, R. L., Helfand, D. J., McMahon, R. G., & Hook, I. M. 1996, AJ, 112, 407
Hewett, P. C., Irwin, M. J., Foltz, C. B., Harding, M. E., Corrigan, R. T., Webster, R. L., & Dinshaw, N. 1994, AJ, 108, 1534
Jacoby, G. H., Hunter, D. A., & Christian, C. A. 1984, ApJS, 56, 257
Keeton, C. R., Kochanek, C. S., & Falco, E. E. 1998, ApJ, 509, 561
Kochanek, C. S. 1992, ApJ, 384, 1
———. 1996, ApJ, 466, 638
Kochanek, C. S., Falco, E. E., Impey, C. D., Lehár, J., McLeod, B. A., & Rix, H.-W. 1998, in AIP Conf. Proc. 470, After the Dark Ages: When Galaxies Were Young, ed. S. S. Holt & E. P. Smith (New York: AIP), 163
Kochanek, C. S., Falco, E. E., & Muñoz, J. A. 1999, ApJ, 510, 590
Kochanek, C. S., & Hewitt, J. N. 1996, Astrophysical Applications of Gravitational Lensing (Dordrecht: Kluwer)
Landolt, A. U. 1992, AJ, 104, 340
Maller, A. H., Simard, L., Guhathakurta, P., Hjorth, J., Jaunsen, A. O., Flores, R. A., & Primack, J. R. 2000, ApJ, 533, 194
Massey, P., Armandroff, T., De Veny, J., Claver, C., Harmer, C., Jacoby, G., Schoening, B., & Silva, D. 1997, Direct Imaging Manual for Kitt Peak (Tucson: NOAO)
McLeod, B. A., Bernstein, G. M., Rieke, M. J., & Weedman, D. W. 1998, AJ, 115, 1377
McMahon, R. G., & Irwin, M. J. 1992, in Digitised Optical Sky Surveys, ed. H. T. MacGillivray & E. B. Thompson (Dordrecht: Kluwer), 417
Monet, D., et al. 1996, USNO-SA1.0 (Washington: US Naval Obs.)
Mortlock, D. J., Webster, R. L., & Francis, P. J. 1999, MNRAS, 309, 836
Muñoz, J. A., Falco, E. E., Kochanek, C. S., & Lehár, J. 1998, ApJ, 492, L9
Narayan, R., & Bartlemann, M. 1998, in Formation of Structure in the Universe, ed. A. Dekel & J. Ostriker (Cambridge: Cambridge Univ. Press), 360
Refsdal, S. 1964, MNRAS, 128, 307
Schechter, P. L., Gregg, M. D., Becker, R. H., Helfand, D. J., & White, R. L. 1998, AJ, 115, 1371
Schechter, P. L., Mateo, M., & Saha, A. 1993, PASP, 105, 1342
Schechter, P. L., & Moore, C. B. 1993, AJ, 105, 1
Steidel, C. C., & Sargent, W. L. W. 1991, AJ, 102, 1610
Turner, E. L., Ostriker, J. P., & Gott, J. R., III. 1984, ApJ, 284, 1
White, R. L., et al. 2000, ApJS, 126, 133
Wisotzki, L., Köhler, T., Kayser, R., & Reimers, D. 1993, A&A, 278, L15